Journal of Environmental Chemical Engineering 13 (2025) 119405

Contents lists available at ScienceDirect

Journal of Environmental Chemical Engineering

journal homepage: www.elsevier.com/locate/jece

Nonradical degradation of antibiotics in seawater by Cl^-/Br^--activated peracetic acid: Dominant contribution of $^1O_2$ and reactive halogens

Jingzhen Su [a], Yong Wang [a,b], Cong Li [a,*], Zhengming He [a], Kai Zhang [a], Mingqiang Ren [a], Qile Wang [a], Tianxing Chen [a], Jibran Ali Ghumro [a], Virender K. Sharma [c], Hyunook Kim [d], Yunshu Zhang [a]

[a] School of Environment and Architecture, University of Shanghai for Science and Technology, Shanghai 200093, China
[b] China Energy Cornerstone Chemical Technology (Shanghai) Co., Ltd., Shanghai 201108, China
[c] College of Engineering, University of Miami, Coral Gables, FL 33124, USA
[d] Department of Environmental Engineering, University of Seoul, Seoul 02504, South Korea

ARTICLE INFO

Keywords:
Br^--PAA system
Cl^--PAA system
Peracetic acid
SMX degradation
Seawater

ABSTRACT

Natural seawater contains abundant halide ions that remain largely untapped, while peracetic acid often requires activation to enhance its oxidative properties. The interaction mechanisms between these components have not been thoroughly investigated. This study investigated the activation effect of high concentrations of Cl^- and Br^- coexisting in seawater on PAA by adding PAA to seawater. Quenching experiments, along with Electron Paramagnetic Resonance (EPR) spectroscopy and UPLC-TQ-MS, were conducted to determine the reaction mechanism and degradation process of SMX. Seawater systems containing 35 ‰ salinity or Br^--PAA systems (0.5 mM Br^-) degraded 100 % SMX within 10 min or 12 min, respectively (k_{obs}=0.4873 min^{-1} or 0.3581 min^{-1}). While the Cl^--PAA system, though slower, still degraded 97.7 % within 180 min (300 mM Cl^-, k_{obs}=0.0173 min^{-1}). SMX degradation rates remained above 95 % across the pH range of 3–9, with optimal performance at pH= 3. However, the presence of HA inhibited SMX degradation efficiency by over 40 %. Results indicate that SMX degradation efficiency correlates positively with Cl^-/Br^- content and PAA concentration. The superior removal efficiency stems from activated PAA not only generating HOCl and HOBr via oxygen atom transfer but also further producing $^1O_2$, which dominates the non-selective degradation process. This approach adapts to a wide pH range but is consumed by coexisting HA. The superiority of the Br^--PAA system over Cl^--PAA stems from the strong oxidizing power of HOBr. The oxidation pathways include halogenation, bond cleavage, and hydroxylation. ECOSAR predictions indicated that most transformation products exhibited higher toxicity than the parent SMX compound.

1. Introduction

The organic peroxyacid (PAA) has found widespread application across various industries, including textile, healthcare, and food processing [1]. Due to its potent bactericidal activity and minimal generation of disinfection byproduct formation, its application in water treatment has become more popular in recent years[2]. Because of its high redox potential (1.06 −1.96 V), PAA is good at oxidizing a variety of micropollutants [3–6]. Reaction rate constants between PAA and various chemicals are reported to vary across nearly 10 orders of magnitude, from 3.2×10^{-6}–1×10^5 $M^{-1}s^{-1}$ [7]. However, the effectiveness of PAA in direct chemical oxidation processes is limited because it can readily oxidize only a few resistant pollutants [6].

PAA is theoretically more readily activated than H_2O_2 and peroxymonosulfate (PMS), as its O−O bond dissociation energy (159 kJ·mol^{-1}) is lower than that of H_2O_2 (213 kJ·mol^{-1}) and PMS (317 kJ·mol^{-1}) [8]. Previous studies have established that external energy sources (e.g., heat [9], UV light [10,11], ultrasound [12]) can activate PAA to degrade organic pollutants or pathogenic microorganisms effectively. However, the introduction of auxiliary energy input leads to additional energy consumption. On the other hand, transition metals and their oxides have also been demonstrated to activate PAA, generating reactive radicals that significantly enhance the degradation efficiency of organic contaminants. For instance, metal ions such as Co^{2+}

* Corresponding author.
E-mail address: licong@usst.edu.cn (C. Li).

https://doi.org/10.1016/j.jece.2025.119405

Available online 20 September 2025

and Fe^{2+} can activate PAA through valence cycling to produce acetylperoxyl radicals ($CH_3C(O)OO\bullet$), enabling rapid degradation of sulfonamide antibiotics. Nevertheless, such systems often face challenges related to metal ion leaching (e.g., Co^{2+} leaching can reach 0.1 −0.5 mg·L^{-1}) [13,14]. Additionally, Co^{2+} may participate in non-target reactions with reactive species generated in the system, thereby reducing the oxidation efficiency [15,16]. Furthermore, recent studies have confirmed that Ru(III) serves as a novel catalyst for PAA activation, exhibiting excellent performance in removing trace-level contaminants from water. However, the high cost associated with the catalyst may limit its large-scale practical application [17]. It is crucial to develop a new PAA activation pathway that is both effective and ecologically benign, as common activation techniques may consume excessive energy and produce secondary pollutants.

Br^- and Cl^- are ubiquitous in seawater and play a key role in chemical oxidation and disinfection. It has been conventionally recognized that Cl^- can form complexes with transition metals (e.g., $FeCl_3^-$), thereby inhibiting catalytic activity. Specifically, in the Fe(II)/PMS system, Cl^- consumes highly reactive $SO_4\bullet^-$, generating less reactive chlorine radicals ($Cl\bullet/Cl_2\bullet^-$), which consequently reduces both the degradation rate and mineralization efficiency of maleic acid [18]. In particular, the presence of Br^- may promote the formation of brominated disinfection byproducts (DBPs) and could lead to excessive consumption of PAA, thereby reducing the utilization efficiency of the oxidant [19]. In addition, Wang et al [20].first identified the dual effect of chloride ions on the decolorization of Orange II in their cobalt-persulfate (Co-PMS) system. Their research indicated that Cl^- in low concentrations (0.05 −10 mM) would hinder decolorization. However, when Cl^- concentration was high (i.e.,>50 mM), the degradation would be significantly accelerated. Such stringent tolerance to salinity variations could significantly restrict its application in complex saline water matrices. In contrast to transition metal-based activation systems, the Cl^-/Br^--activated process operates without the requirement of an external catalyst. Studies have shown that ~~halide ions~~ Cl^- act as PMS activators to generate active reactive species. Lou et al [21]. demonstrated effective degradation of Rhodamine B (RhB) via direct activation of PMS by chloride ions. However, this system requires an exceedingly high chloride ion concentration (120 mM) to achieve efficient degradation under acidic conditions (pH=3), implying a dependency on high-salinity water environments. Moreover, Li et al [22]. focused particularly on the influence of pH on the activation of PMS by Cl^-, highlighting that the degradation process is dominated exclusively by a non-radical pathway (involving HOCl) under acidic conditions. In contrast, a radical-based pathway becomes operative at neutral pH, albeit with significantly reduced degradation efficiency, thereby limiting its practical applicability in natural water matrices. Liu et al [23]. proposed that the activation of PAA by Br^- yields HOBr as the sole "secondary oxidant," which degrades bisphenol A (BPA) via electrophilic substitution reactions. However, their interpretation neglects the potential contribution of PAAs intrinsic activation pathways, which may generate additional reactive species and play a role in the degradation process. Currently, most studies have overlooked both the potential and the mechanisms of halide ions as activators of PAA under specific conditions, particularly within seawater systems. To elaborate further, direct utilization of seawater-borne chloride and bromide for PAA activation to remove antibiotics represents a context-appropriate strategy. Such an approach not only aligns with the principles of China's "14th Five-Year Plan for Marine Ecological Environmental Protection" by mitigating coastal pollution without introducing ecotoxic risks to marine organisms, but also offers significant advantages in reducing operational costs and minimizing secondary pollution [24]. On one hand, this strategy facilitates the resource utilization of halides, offering economic and environmental benefits while actively responding to the "Carbon Dioxide Peaking Action Plan Before 2030" issued by the State Council of China [25]. It thereby contributes to sustainable development. On the other hand, compared to the PMS-halide system [20], the synergistic mechanism among reactive species proposed in this study demonstrates stronger applicability in high-salinity environments.

SMX is a common antibiotic used in aquaculture, animal husbandry, and healthcare [26]. Since SMX cannot be fully metabolized by humans and animals, it is unavoidable for its unmetabolized portion to be released into the water environment. Because of its strong chemical stability and possible antibacterial qualities, leftover SMX can be released without adequate treatment, which poses a serious risk to the environment and public health by encouraging the growth of bacteria that have genes resistant to antibiotics [27]. However, it is challenging to eliminate SMX and its potential dangers from water using traditional treatment processes.

This study focuses on the degradation of SMX. The degradation effect of Cl^-/Br^--PAA system and seawater system on SMX was evaluated, and the active species in the system were identified by EPR and quenching experiments. The influence of anions, HA, pH, etc., in water bodies on the degradation capacity of the oxidation system is studied. The applicability of the oxidation system to four different pollutants is evaluated. In addition, the reaction mechanism and degradation pathway of active halogen species with SMX were studied by combining DFT. And the toxicity of SMX after degradation was tested.

2. Materials and methods

2.1. Chemicals and materials

All of the compounds utilized in this investigation are analytical grade or above. All chemical solutions are prepared by using deionized water created by Plus-E3 (EPED, Shanghai, China). PAA (>15 % w/w), SMX, Ciprofloxacin (CIP), Sulfadimethoxine (SMT), Triclosan (TCS), Tetracycline hydrochloride (TH), sodium chloride (NaCl, 99.9 %), sodium bromide (NaBr), humic acid (HA), potassium iodide (KI), sodium thiosulfate standard solution ($Na_2S_2O_3$, 1 mM), magnesium chloride ($MgCl_2$), potassium chloride (KCl), calcium chloride ($CaCl_2$), strontium chloride ($SrCl_2$), magnesium sulfate ($MgSO_4$), furfuryl alcohol (FFA), tert-butyl alcohol (TBA), Benzoic acid (BA), 2,4-Hexadiene (2,4-HD), ammonium sulfate ($(NH_4)_2SO_4$), ammonium molybdate ($(NH_4)_2MoO_4$), 5,5-dimethyl-2-pyrrolidone-N-oxyl (DMPO) and 2,2,6,6-Tetramethyl-1-piperidinyloxy (TEMP) were obtained from Aladdin (Shanghai, China). Sulfuric acid (H_2SO_4), sodium hydroxide (NaOH), sodium bicarbonate ($NaHCO_3$), sodium hypochlorite solution (NaOCl, 6 −14 % active chlorine basis), p-benzoquinone (p-BQ) and soluble starch were obtained from Macklin (Shanghai, China). Hydrogen peroxide (H_2O_2, 30 % w/w), sodium sulfate (Na_2SO_4), manganese sulfate ($MnSO_4$), and potassium permanganate ($KMnO_4$) were supplied by Sinopharm Chemical Co. LTD (China, >99 % purity). Acetonitrile (CH_3CN) and methanol (CH_3OH, MeOH) were purchased from Adamas-Beta LTD (Shanghai, China). Free chlorine reagent powder pillow was purchased from HACH (China).

2.2. Experimental procedures

A 100 mL aliquot of 0.02 mM SMX solution was placed in a 250 mL conical flask, followed by sequential addition of NaCl (25 −300 mM), NaBr (0.125 −2.0 mM) and PAA (0.25 −2 mM). Furthermore, conduct seawater simulation experiments with salinity of 5 ‰−35 ‰ (Table S1). All experiments were conducted under continuous magnetic stirring at 25 ± 1°C, 300 rpm, and sampled at predetermined intervals. Each test aliquot was collected and free chlorine was measured immediately by DPD reagent. Subsequently, it was quenched with excess $Na_2S_2O_3$. Referring to the above operations, SO_4^{2-} (0 −4 mM), HA (0 −50 mg·L^{-1}) and HCO_3^- (0 −2 mM) were added to explore the influence of water quality. The original pH of the solution was adjusted using 10 mM H_2SO_4 and 10 mM NaOH. Excessive quenchers such as MeOH, TBA, p-BQ, FFA, 2,4-HD, BA and $(NH_4)_2SO_4$ were added to verify the reaction system. To ensure data reliability, all experimental runs were performed in three

independent replicates. The results are reported as the mean±standard deviation, unless otherwise stated.

2.3. Analytical and simulation methods

Spectrophotometry was used to measure the peroxides left behind after each reaction, and iodometric and potassium permanganate titration techniques were used to periodically calibrate PAA solutions. Free chlorine was determined by spectrophotometrically using DPD reagent (DR2800, HACH, Colorado, USA). Free bromine was determined by spectrophotometry. The SMX concentrations were measured using a high-performance liquid chromatograph (HPLC) (LC-2030, Shimadzu, Kyoto, Japan) with a C18 column (5 μm, 4.6 mm×250 mm). The injection volume was set at 15 μL, the temperature of the column was set at 35 ℃, and the flow rate was set at 0.5 mL·min^{-1}. 60 % acetonitrile and 40 % ultrapure water made up the mobile phase. 257 nm was chosen as the SMX wavelength. Intermediate products from SMX oxidation were detected using UPLC-TSQ-MS (TSQ Quantis, Thermo Fisher, Massachusetts, USA), Total organic carbon (TOC) was determined using a TOC/TN analyzer (Multi N/C3100, Analytik Jena, Jena, Germany). The relevant experimental flowchart is provided in Fig. S1 of the Supplementary Materials. The degradation kinetics of SMX were modeled using pseudo-first-order kinetics. The k_{obs} was determined by linear regression of the plot of -ln(C_0/C_t) versus time. All kinetic fittings were performed using Origin 2024 software.

Gaussian 16 W software was used in this study to perform theoretical calculations based on DFT. Taking into account solvent effects, the SMD solvation model (in water) was used for all calculations and geometry optimization was performed at the M062X/6–31 G(d) level. Subsequent computations were subsequently carried out at the same level using the SMX molecule's most stable state and ideal geometrical shape. Calculation of front orbital energies of SMX molecules was performed by the Multiwfn program which is based on the Hirshfeld approach. The initial structure of the SMX molecule prior to geometric optimization was obtained from the PubChem database (CID: 5329).

3. Results and discussion

3.1. Evaluation of PAA oxidation system based on Cl^- and Br^-

PAA solutions usually contain H_2O_2 [28]. Five systems, including Cl^--PAA, were constructed to degrade SMX (Fig. 1a). Control experiments confirmed minimal SMX degradation by Cl^-, PAA, H_2O_2 or Cl^--H_2O_2 alone (<10 % removal), whereas the Cl^--PAA system achieved 97.7 % removal and the k_{obs} value was 0.0173 min^{-1} (Fig. S2a), indicating that H_2O_2 in the Cl^--PAA system could not degrade SMX, but the coupling effect of Cl^- and PAA was observed. Compared with H_2O_2, Cl^- is easier to activate PAA to produce highly active species. This phenomenon can be attributed to the significantly lower bond dissociation energy (BDE) of the O−O bond in peracetic acid (170 kJ/mol) compared to that in hydrogen peroxide (220 kJ/mol). In addition, the concentration of HOCl detected in the system varies with the reaction time. Specifically, after 180 min of reaction, PAA consumed 0.46 mM, but only generated 0.021 mM HOCl, indicating that HOCl would directly react with SMX [29,30]. Five different systems, such as Br^--PAA, were constructed to degrade SMX (Fig. 1b). The degradation effect of single Br^-, PAA, H_2O_2 or Br^--H_2O_2 systems on SMX was weak, while SMX was removed entirely in the Br^--PAA system, with the maximum k_{obs} value of 0.3581 min^{-1} (Fig. S2b), indicating that the entire reaction system mainly degraded SMX by the coupling effect of Br^- and PAA, and Br^- may also activate PAA to produce highly active species.

In addition, Cl^- and Br^- are ubiquitous in water bodies, especially in seawater, with concentrations of up to 20 g·L^{-1} and 0.067 g·L^{-1}, respectively [31,32]. Therefore, artificial simulated seawater was prepared as a medium to degrade SMX. The results showed that SMX could be removed entirely (Fig. 1c), and the reaction conformed to

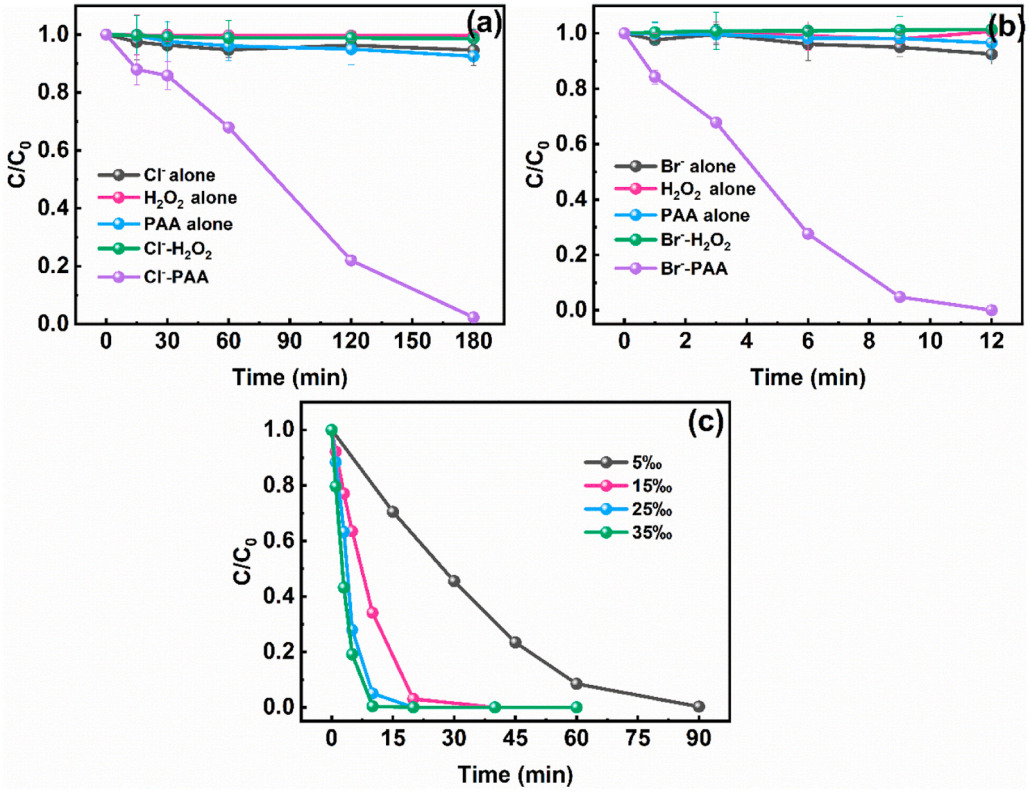

Fig. 1. (a), (b), and (c) are the time distributions of SMX concentrations in different reaction systems ($[Cl^-]_0$=300 mM, $[Br^-]_0$=0.5 mM, $[H_2O_2]_0$=$[PAA]_0$=1 mM, $[SMX]_0$=0.02 mM).

pseudo-first-order reaction kinetics (Fig. S2c). The high removal efficiency can be attributed to the rapid reaction between Br^- and free chlorine ($HOCl/OCl^-$) to form free bromine ($HOBr/OBr^-$) when Cl^-, Br^- and PAA coexist (Eqs 1 −2). Notably, in seawater system (salinity 35 ‰), 100 % of SMX degradation was achieved within 10 min, demonstrating superior performance compared to the Cl^-/Br^--PAA system alone, and free bromine enhances the degradation effect. Other related reactions that may occur during the degradation process are shown in Table 1.

3.2. Active substances and oxidation mechanisms in different oxidation systems

3.2.1. Formation of singlet oxygen

To verify the predominant reactive species and degradation mechanisms, controlled quenching experiments and comparative system analyses were performed. Significant inhibition of SMX degradation was observed following FFA addition to the oxidation system (Figs. 2a and 2b), indicating that $^1O_2$ was both present and the predominant reactive species. However, Song et al[35]. proposed that in the Cl^--PAA system, carbon-centered radicals (e.g., $CH_3C(=O)OO\bullet$ and $CH_3C(=O)O\bullet$) along with Cl_2/HClO were the dominant reactive species, and no $^1O_2$ was detected. This discrepancy can be attributed to differences in both contaminant structure and reaction conditions. Specifically, Song et al. employed BPA as the target compound, whose high electron density on the aromatic ring makes it highly susceptible to attack by carbon-centered radicals. In contrast, the SMX molecule investigated in this study contains a sulfonamide group ($-SO_2NH-$), which is more prone to selective oxidation by $^1O_2$ at electron-rich sites. Furthermore, the PAA concentration used in our study (0.25–2 mM) was significantly lower than that applied by Song et al. (20–40 mM). Under such low PAA concentrations, the generation of carbon-centered radicals is limited, thereby further enhancing the dominant role of $^1O_2$ in the low-dose PAA system. Therefore, different ClO^- reaction systems were constructed to explore the source of $^1O_2$ in the Cl^--PAA system (Fig. 2c). Control experiments revealed that NaClO alone (containing 0.45 mM HOCl) achieved only 20 % SMX degradation, demonstrating that $^1O_2$ generation did not originate from HOCl self-decomposition. The enhanced degradation performance observed in the Cl^--NaClO system compared to NaClO alone can be attributed to excess Cl^- reacting with HOCl to generate additional oxidants, particularly soluble Cl_2. The Cl^--NaClO--PAA system achieved an exceptional SMX degradation efficiency of 98.7 % with an observed k_{obs} value of 0.0213 min^{-1} (Fig. S3c), demonstrating superior oxidation capability. The current system exhibits functional equivalence to a Cl^--PAA system, demonstrating comparable SMX degradation performance to the Cl^--PAA system. It is noteworthy that the high degradation efficiency observed in the Cl^--PAA system is contingent upon the transfer of an oxygen atom from PAA to Cl^-, leading to the formation of HOCl. This mechanism is consistent with the findings reported by Zhou et al[39].

Single PAA cannot degrade SMX for the Cl^--PAA system, eliminating the possibility of $^1O_2$ production via PAA self-decomposition in the Cl^--PAA system. Neither continuous N_2 purging (to remove dissolved oxygen) nor adding p-BQ inhibited SMX degradation (Fig. 2a), indicating that $O_2\bullet^-$ and dissolved oxygen played negligible roles in $^1O_2$ generation or the overall degradation process. So, in the Cl^--PAA system, the degradation mechanism proceeds through three key steps: (i) initial reaction between Cl^- and PAA to generate HOCl (Eq. 3), (ii) conversion of HOCl to Cl_2 in the presence of excess Cl^- (Eq. 4), followed by (iii) Cl_2-mediated cleavage of the PAA O−O bond to yield $^1O_2$ (Eq. 5). Similar to the Cl^--PAA system, HOBr is generated in situ by Br^- through the transfer of PAA oxygen atoms, and then HOBr reacts with PAA to break its peroxide bond (O−O) and release $^1O_2$ (Eq. 11). No excess Br^- is required to participate in the formation of Br_2 intermediates, and the reaction kinetics are faster.

3.2.2. Other active species in the oxidation system

The presence of HOCl, HOBr and various radical species in the system were quantitatively confirmed through quenching experiments The role of radical species was investigated through quenching experiments (Figs. 3a, and 3b). MeOH was first added to the Cl^--PAA system to quench •OH and RO• [40], The results showed that 11 % of SMX degradation was inhibited and the k_{obs} value was decreased (Fig. S4a). When TBA was subsequently introduced, only minimal degradation inhibition was observed, demonstrating that while •OH radicals were present, they played a negligible role in SMX degradation. Different quenching patterns emerged in the Br^--PAA system. MeOH addition inhibited 36 % of SMX degradation, suggesting greater radical involvement. However, the addition of 2,4-HD caused more than 70 % inhibition in both Cl^--PAA and Br^--PAA systems, which was inconsistent with the results obtained when MeOH was used as a RO• quencher.

With reference to quenching experimental results, quantitative analysis of residual HOCl in the Cl^--PAA system (Fig. S4c) revealed that 2,4-HD addition reduced HOCl levels by 95 %, demonstrating its consumption of HOCl rather than solely quenching RO•. This phenomenon can be attributed to the electrophilic addition reaction between HOCl

Table 1
Possible reaction in different oxidative systems.

System	Step	Reaction	Notes	Ref.
Artificial seawater system	HOBr generation	$HOCl+Br^-\rightarrow HOBr+Cl^-$ (1)	Acidic environment	[33]
	OBr^- generation	$OCl^-+Br^-\rightarrow OBr^-+Cl^-$ (2)	Alkaline environment	
Chloride-PAA	HOCl generation	$Cl+CH_3C(O)OOH\rightarrow HOCl+CH_3C(O)O^-/CH_3C(O)O\bullet$ (3)	Cl^- direct activation of PAA/free radical intermediates	[34, 35]
	Cl_2 generation	$HOCl+H^++Cl^-\rightleftharpoons Cl_2(aq)+H_2O$ (4)	Cl^- excess	[36]
	$^1O_2$ generation	$Cl_2+CH_3C(O)OOH+H_2O\rightarrow {}^1O_2+2Cl^-+2H^++CH_3C(O)OH$ (5)	Non-Free radical	[37]
	Cl• generation	$Cl^-+H^++\bullet OH\rightarrow Cl\bullet+H_2O$ (6) $Cl^-+CH_3C(O)O\bullet+H^+\rightarrow Cl\bullet+CH_3C(O)OOH$ (7)		
Bromide-PAA	HOBr generation	$Br^-+\bullet OH\rightarrow Br\bullet+OH^-$ (8) $Br\bullet+\bullet OH\rightarrow HOBr$ (9) $Br^-+CH_3C(O)OOH\rightarrow CH_3C(O)O-+HOBr$ (10)	Free radical chain reaction, electron transfer Free radical recombination reaction In situ generation of HOBr by Oxygen Atom Transfer	[32]
	$^1O_2$ generation	$HOBr+CH_3C(O)OOH\rightarrow {}^1O_2+Br^-+CH_3C(O)OH+H^+$ (11)	Non-Free radical	
Shared steps(PAA)	Free radical chain reaction	$CH_3C(O)OOH\rightarrow CH_3C(O)O\bullet+\bullet OH$ (12) $CH_3C(O)OOH+CH_3C(O)O\bullet\rightarrow CH_3C(O)OO\bullet+CH_3C(O)OH$ (13) $CH_3C(O)OOH+\bullet OH\rightarrow CH_3C(O)OO\bullet+H_2O$ (14) $2CH_3C(O)OO\bullet\rightarrow 2CH_3C(O)O\bullet+O_2$ (15)	PAA decomposition generates radicals Free radicals can be transferred and increased •OH abstracts H From PAA Continue to expand the number of Free radicals and the reaction range	[2]
Other reactions	Cl• is quenched	$HCO_3^-+Cl\bullet\rightarrow CO_3^{\bullet-}+HCl$ (16)	HCO_3^- exist	[38]

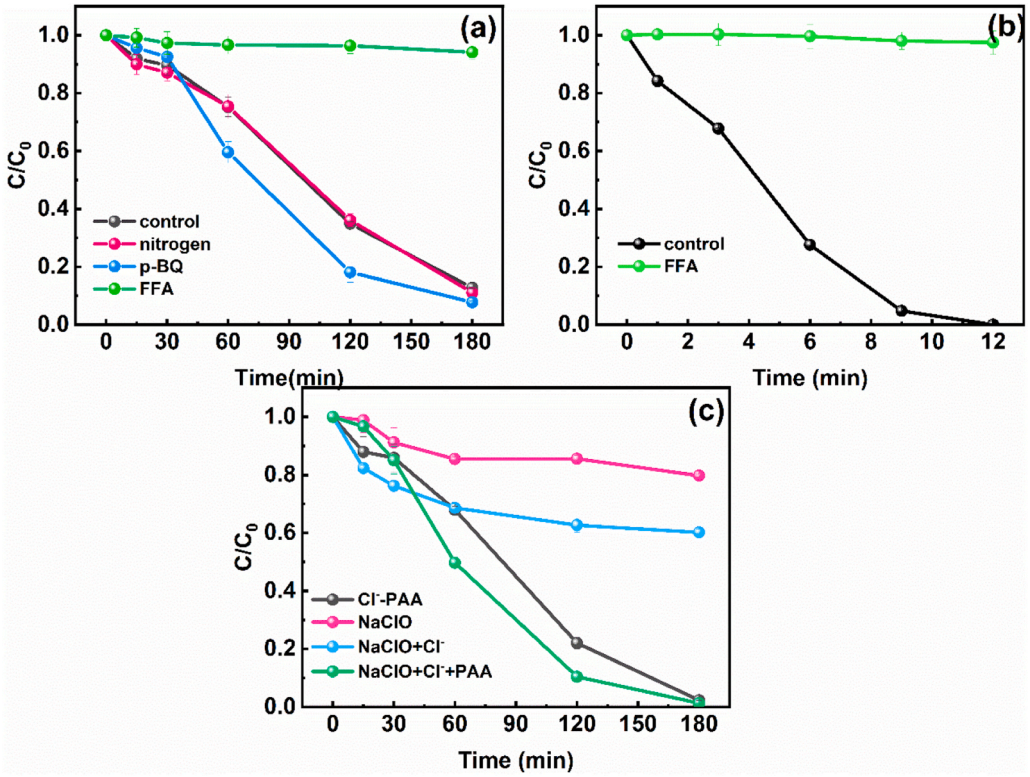

Fig. 2. (a) Effects of p-BQ, FFA and Nitrogen purge on the degradation of SMX in Cl^--PAA system, (b) Effect of FFA on the degradation of SMX in Br^--PAA system, (c) Removal of SMX by different systems containing ClO^- ($[Cl^-]_0$=300 mM, $[Br^-]_0$=0.5 mM, $[PAA]_0$=1 mM, $[SMX]_0$=0.02 mM, [HOCl]=0.45 mM, $[p\text{-}BQ]_0$ =10 mM [24], $_0$=2 mM).

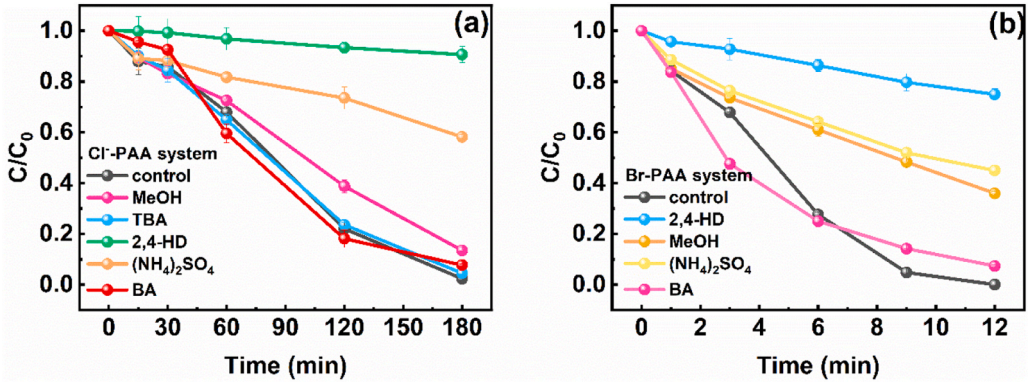

Fig. 3. SMX removal extents over time in the presence of different oxidant scavengers: (a) Cl^--PAA system, (b) Br^--PAA system ($[Cl^-]_0$=300 mM, $[Br^-]_0$=0.5 mM, $[PAA]_0$=1 mM, $[SMX]_0$= 0.02 mM, $[2,4\text{-}HD]_0$=2 mM, $[MeOH]_0$=$[TBA]_0$=$[(NH_4)_2SO_4]_0$= 20 mM, $_0$[14]= 10 mM).

and the dual C=C bonds in 2,4-HD, facilitated by the strong oxidative capacity of HOCl. When NH_4^+ was added to the both systems, 57 % of SMX degradation was inhibited in the Cl^--PAA system, and HOCl was reduced by 76 %, which also shows the effect of HOCl on SMX degradation. Similarly, 55 % of SMX degradation was inhibited in the Br^--PAA system, indicating that HOBr has a greater effect on SMX degradation. While PMS systems are known to oxidize Br^- to Br• via electron transfer (Eq. 8), with subsequent HOBr formation through •OH reaction (Eq. 9). BA quenching experiments revealed negligible SMX degradation inhibition. This absence of BA-sensitive activity unequivocally excludes Br• as a reactive intermediate in the Br^--PAA system. Instead, HOBr is generated in situ through PAA OAT to Br^- (Eq. 10), a mechanism that will be validated in Section 3.3. Furthermore, this observation is consistent with the core conclusion reported by Du et al [41]. that PAA oxidizes Br^- to form HOBr. However, a key difference lies in our finding that HOBr can further transform into $^1O_2$, thereby introducing a non-radical oxidation pathway. In contrast, Du et al. proposed a reaction mechanism dominated primarily by electrophilic bromination rather than involving radical or energy transfer pathways such as $^1O_2$.

3.2.3. *Electron paramagnetic resonance spectroscopic analysis*

EPR spectroscopy was employed to detect reactive oxygen species, with DMPO as the spin-trapping agent for •OH and TEMP for $^1O_2$ [42]. The free radical species generated by the oxidation system were further verified (Fig. 4a). No radical signals were detected in the initial EPR spectra (0 min) for either DMPO alone or PAA alone. After 15 min of reaction, distinct 5,5-dimethyl-2-pyrrolidone-N-oxyl (DMPOX) signals emerged, confirming the generation of organic radicals (e.g., RO•, $CH_3C(O)O$•). However, these signals showed significant attenuation by 30 min, suggesting radical quenching or transformation over time. A

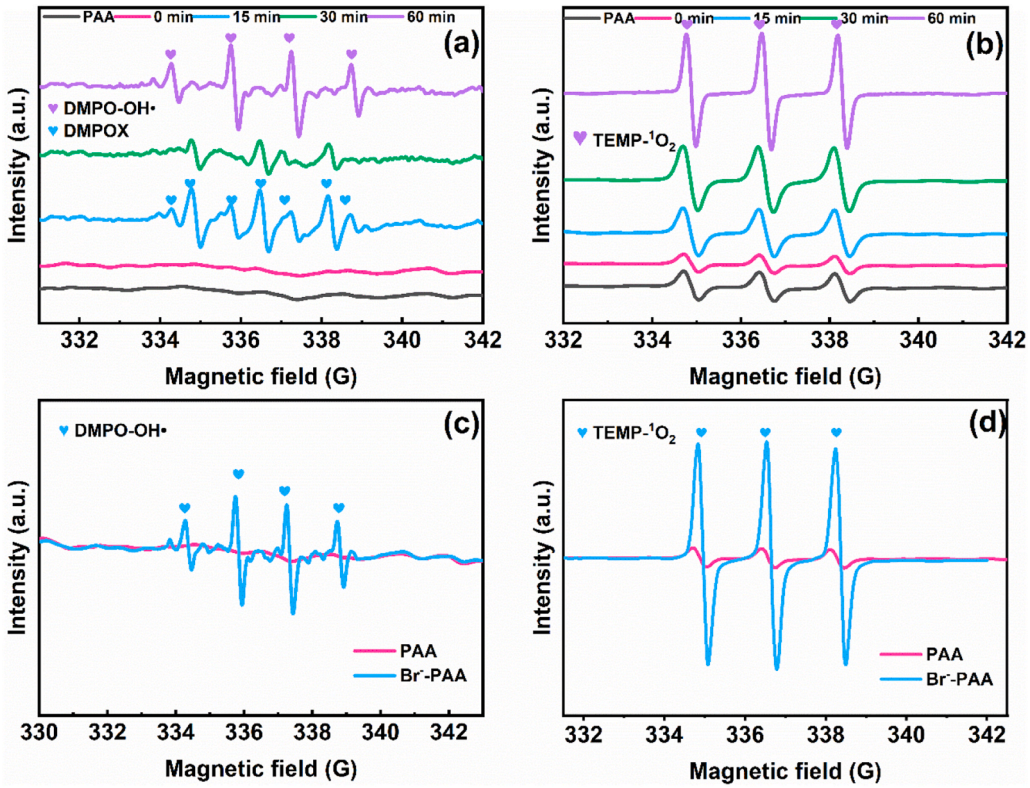

Fig. 4. EPR spectra of DMPO and TEMP obtained at different time intervals: (a) and (b) are Cl^--PAA system, (c) and (d) are Br^--PAA system ($[Cl^-]_0$=300 mM, $[Br^-]_0$=0.5 mM, $[PAA]_0$=1 mM, $[SMX]_0$=0.02 mM, $[DMPO]_0$=50 mM, $[TEMP]_0$=50 mM).

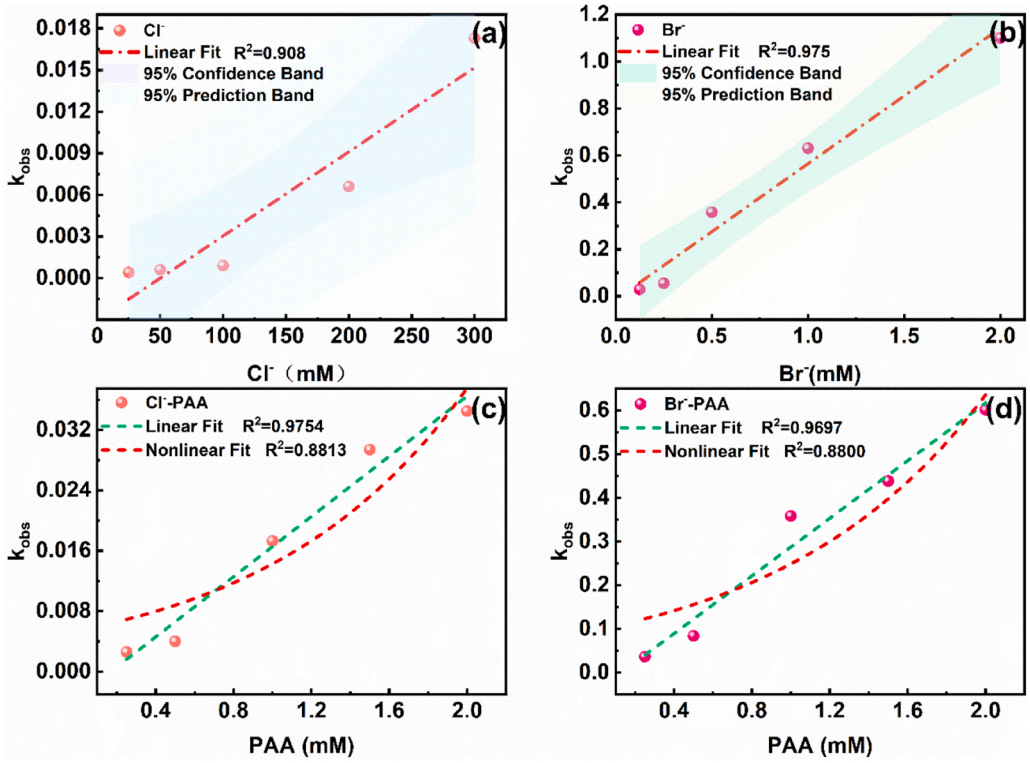

Fig. 5. (a) and (b) are the correlations between Cl^-/Br^- concentration and the k_{obs} value of SMX degradation, (c) and (d) are the relationships between PAA concentration and SMX removal in the Cl^-/Br^--PAA system ($[Cl^-]_0$=300 mM, $[Br^-]_0$=0.5 mM, $[H_2O_2]_0$=$[PAA]_0$=1 mM, $[SMX]_0$=0.02 mM).

distinct •OH signal was was detected by EPR at 60 min [43]. The results show that Cl^- can activate PAA to produce •OH and RO•. Figs. 4b and 4d confirm $^1O_2$ production in both oxidation systems. Notably, while the Br^--PAA system showed detectable •OH signals (Fig. 4c), no characteristic RO• signals were observed, consistent with the quenching experimental results. In summary, we can determine that $^1O_2$ is generated in the oxidation system. While weak signals corresponding to $CH_3C(O)O$• and related radicals were detected (Eqs. 12 −15), their minimal intensity indicates that PAA alone contributes negligibly to the overall degradation process.

3.3. Influencing factors

3.3.1. Cl^-/Br^- and PAA concentrations

Systematic evaluation of halide ion concentrations revealed distinct activation behaviors in the oxidative systems (Figs. S4a and S4e). The Cl^--PAA system exhibited optimal performance at 300 mM Cl^-, achieving 97.7 % SMX removal. In contrast, the Br^--PAA system demonstrated superior activation kinetics, with complete SMX degradation attained within 12 min at 0.5 mM Br^-. Notably, increasing Br^- concentration to 2 mM further accelerated the process, reducing the required treatment time to merely 3 min. These comparative results unequivocally establish Br^- as a more efficient activator than Cl^- for PAA-mediated SMX degradation. Regression analysis revealed a strong correlation between Cl^-/Br^- concentration and the k_{obs} value for SMX degradation (Figs. 5a and 5b). Excess Cl^- accelerated PAA activation, promoting Cl_2 generation through Eqs. 3 −4. When Eq. 4 became the dominant pathway, the rapid consumption of PAA led to substrate depletion, consequently slowing SMX degradation rates. The Br^--PAA system exhibited higher activation efficiency than Cl^--PAA, which was due to the stronger oxidizing property of HOBr than that of HOCl. Our results demonstrate that Cl^-/Br^- concentrations critically govern PAA activation for SMX degradation, with the k_{obs} value showing positive linear correlation within specific concentration ranges (Fig. S6b and 6d). This finding is consistent with the conclusion reported by Huang et al [44].

Additionally, Figs. 5c and 5d demonstrate significant correlations between SMX degradation rates and PAA concentration (R^2> 0.96 for linear fitting, R^2> 0.88 for nonlinear fitting), confirming that direct PAA activation by halides (Eqs. 3, 10) to generate HOCl/HOBr dominated the oxidation process, as further supported by Fig. S6d. Higher PAA concentrations increased:(i) Collision frequency with Cl^-/Br^-, accelerating reaction rates (Fig. S5e, 5 g), and (ii) Suppression of side reactions (e.g., Cl_2/Br_2 hydrolysis), ensuring efficient HOCl/HOBr conversion. At the same time, the degradation of k_{obs} by SMX is exponentially related to the PAA concentration (R^2≥0.88), indicating that there is a free radical chain reaction in the system but it is not dominant, and the results are consistent with the quenching experiment and EPR analysis.

3.3.2. pH

The Cl^--PAA system achieved > 95 % SMX removal in the pH range from 3 to 9, with partial inhibition observed at pH= 11 (Figs. 6a, S5a). Under acidic conditions (pH ≤6), HOCl formation dominated, and excess Cl^- promoted its rapid conversion to Cl_2 (Fig. S6c). As a strong electrophile, Cl_2 preferentially oxidizes electron-rich moieties in SMX, while coexisting $^1O_2$ further enhanced degradation. When pH> 6, OCl^- gradually increases and the oxidizing property weakens. Although PAA is homolytically cleaved to generate $CH_3C(O)O$• and •OH under alkaline conditions (eq 12), the amount generated is small and some free radicals will be quenched by Cl^-. Similar to the Cl^--PAA system, the Br^--PAA system achieved > 95 % SMX removal in the pH range from 3 to 11, Under alkaline conditions, its inhibitory effect is weaker (Fig. 6b). In contrast, Zhao et al[45]. reported that the HOBr generated in the Br^--PMS system efficiently degrades TCS only at pH 7.0, as PMS tends to undergo self-decomposition under pH deviations. However, the PAA-based system offers distinct advantages: on one hand, PAA can buffer the initial alkaline pH; on the other hand, given its high pKa value of 8.2, the neutral form of PAA (1.75 V vs. SHE), which predominates at pH< 8.2, exhibits stronger oxidative capacity than the anionic form (PAA^-, 1.01 V vs. SHE). These properties collectively minimize the

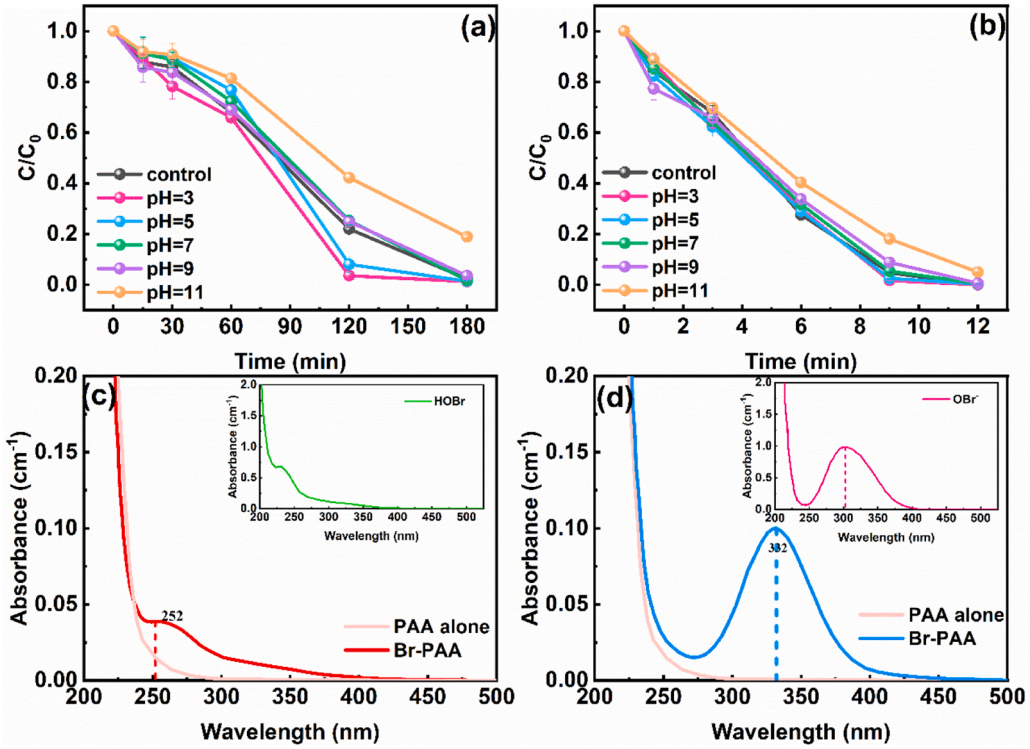

Fig. 6. (a) Effect of pH on the degradation of SMX in Cl^--PAA system, (b) Effect of pH on the degradation of SMX in Br^--PAA system, (c) UV absorption spectrum of HOBr at pH= 7, (d) UV absorption spectrum of OBr^- at pH= 11 ($[Cl^-]_0$=300 mM, $[PAA]_0$=1 mM, $[Br^-]_0$=0.5 mM, $[HOBr]_0$=2.5 mM).

influence of pH variations. Moreover, even though HOBr dissociates into the less reactive OBr^- under alkaline conditions, this loss of reactivity is compensated by the conversion of HOBr to $^1O_2$. As a result, the initial alkaline pH exhibits no significant inhibitory effect on the degradation of SMX. This marked difference from conventional systems primarily stems from the combined effect of PAA's species distribution advantage and its inherent buffering capacity.

Fig. 6c shows that at pH= 7, the single PAA system has no characteristic peak above 250 nm, while the Br^--PAA system has an absorption peak at 252 nm. The peak position is offset but overall it is consistent with the UV spectrum of HOBr, proving that HOBr is generated in the PAA solution in the presence of Br^-,while pH= 11 produced an OBr^--specific peak at 332 nm (Fig. 6d) [46]. DFT simulations (Figs. S5d, S6) corroborated these results: it is reasonable that HOBr is mainly present under neutral conditions (the peak position is offset but the overall UV spectrum is consistent with HOBr) [23]. The absorption peak under alkaline conditions (with OH^-) is closely related to OBr^-, and after adding water molecules, it is more similar to the experimental result (332 nm). If OBr^- and HOBr coexist in water, the peak will shift significantly (405 nm). This pH-dependent speciation (HOBr dominance at pH≤7 versus OBr^- at pH≥11) critically governed oxidative efficiency, as the lower redox potential of OBr^- compared to HOBr reduced degradation rates under alkaline conditions.

3.3.3. Coexisting substances

The effects of SO_4^{2-}, HA, and HCO_3^- in natural water on the degradation of SMX in the Cl^--PAA system were investigated (Fig. 7a). SO_4^{2-} showed negligible influence on SMX degradation with only a slight decrease in k_{obs} (Fig. S8a), as •OH quenching by excess SO_4^{2-} [12], but •OH contributes negligibly to SMX degradation in the Cl^--PAA system. HA (50 mg·L^{-1}) significantly inhibited SMX degradation (58.5 % remaining, k_{obs}=0.001 min^{-1}, Fig. S8c) through multiple pathways: quenching •OH/RO• and reacting with free chlorine/$^1O_2$ [47]. This observation differs from the findings reported by Wang et al[48]. regarding the enhancing effect of NOM on Cu(II)-activated PAA, indicating that the influence of NOM on the reaction is highly dependent on the dominant reactive species in the system as well as the strength of interaction between NOM and the reactive species/catalyst. HCO_3^- inhibition primarily occurred via $^1O_2$ scavenging [49], though its additional potential to quench Cl• (k = 8.5 ×10^6 $M^{-1}s^{-1}$, Eq. 16) was ruled out by BA experiments (k = 1.8 ×10^{10} $M^{-1}s^{-1}$) showing no Cl• involvement (Fig. 3a) [50], confirming $^1O_2$ as the main affected species. These results demonstrate that while SO_4^{2-} is negligible, both HA and HCO_3^- substantially interfere with the Cl^--PAA process, mainly through $^1O_2$ consumption.

In the Br^--PAA system, SO_4^{2-} had a weak inhibitory effect on SMX degradation (Fig. 7b). In contrast, HA significantly suppressed SMX degradation through two synergistic mechanisms: (i) competition with SMX as an electron donor via its reducing functional groups, and (ii) consumption of free bromine (k_{obs}=15 −167 $M^{-1}s^{-1}$)[51]. which collectively diminished oxidative efficiency. HCO_3^- inhibited the degradation of SMX, and similar to Cl^--PAA, the inhibition of $^1O_2$ was taken into account. These results collectively demonstrate that coexisting substances predominantly impair oxidation efficiency by depleting key reactive species (free bromine, $^1O_2$) or competing for oxidation sites. This finding provides a clear direction for practical water pretreatment strategies: priority should be given to the removal of humic acid (HA) (e.g., via coagulation-adsorption processes), which may lead to a reduction in operational costs.

3.4. Evaluation of the degradation effect of other antibiotic pollutants

The study further expanded its scope by selecting four representative antibiotics (CIP, TH, TCS, and SMT) as target contaminants to comprehensively evaluate the applicability of the Cl^-/Br^--PAA oxidation system. The results revealed distinct degradation selectivity among these compounds, highlighting the system's differential oxidation capacity for various antibiotic classes: CIP (12.0 %), TH (77.2 %), TCS (72.6 %), and SMT (14.8 %) removal in the Cl^--PAA system, compared to CIP (11.5 %), TH (33.5 %), TCS (33.0 %), and SMT (16.6 %) in the Br^--PAA system (Fig. S9).

The ionization potential (IP) of organic compounds can be used as an indicator to evaluate the redox ability of the oxidation system [52]. DFT simulation was further used to calculate the IP values of four pollutants, which were defined as low ionization potential (IP<8) and medium ionization potential (8 <IP<9) [53]. A clear correlation was established between pollutant ionization potential (IP) and degradation kinetics (k_{obs}) (Fig. 8). The Br^--PAA system demonstrated superior oxidation capacity for pollutants with higher IP values (TH, TCS, SMT), though their absolute removal rates remained limited by the system's reaction time. At the same time, SMX with a lower IP value was easily degraded and negatively correlated with the IP value, which indicated that the oxidation system was more dependent on nonradical pathways [54,55]. This mechanistic interpretation is further supported by the known selectivity of $^1O_2$ for electron-rich phenolic compounds. This also proves the existence of $^1O_2$ in the Cl^-/Br^--PAA system, making halogen-activated PAA a selective oxidation technology for water purification.

3.5. Degradation pathway

DFT calculations were performed to characterize the electronic properties of SMX, including electrostatic potential (ESP) mapping (Fig. S10b), frontier molecular orbital distributions (HOMO and LUMO,

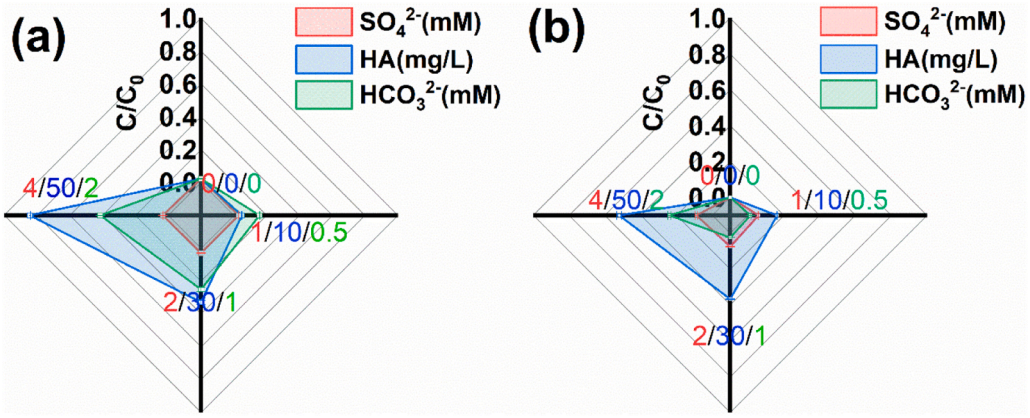

Fig. 7. Effects of SO_4^{2-}, HA and HCO_3^-: (a) Cl^--PAA system, (b) Br^--PAA system ($[Cl^-]_0$=300 mM, $[Br^-]_0$=0.5 mM, $[PAA]_0$=1 mM, $[SMX]_0$=0.02 mM, $[SO_4^{2-}]_0$=0 −4 mM, $[HCO_3^-]_0$=0 −2 mM, $[HA]_0$=0 −50 mg·L^{-1}).

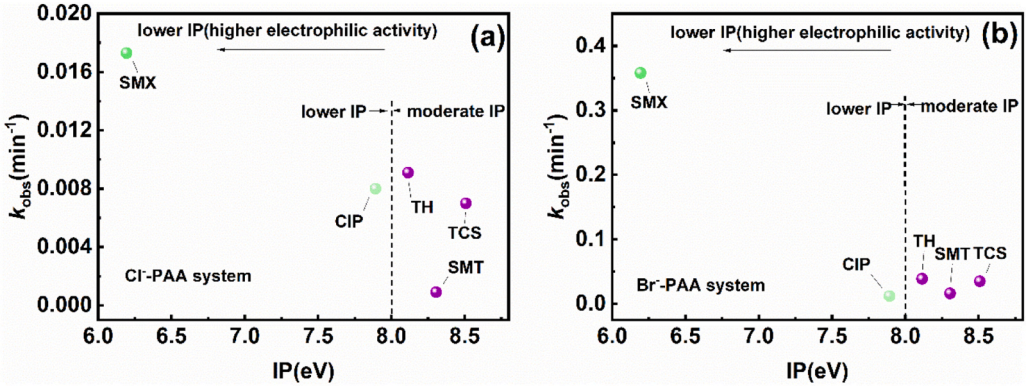

Fig. 8. The relationship between organics degradation rates and their ionization potentials (IP): (a) Cl^--PAA system,(b) Br^--PAA system ($[Cl^-]_0$=300 mM, $[Br^-]_0$=0.5 mM, $[PAA]_0$=1 mM, $[pollutants]_0$=0.02 mM).

Figs. S9c,d), and condensed Fukui functions (f^-, f^0; Figs. S9e,f). It was found that electron-rich atoms (i.e., N11, N17, C1, and C5) are located in areas where the HOMO orbital is concentrated, suggesting that these positions are most susceptible to oxidation and electron loss [56]. The LUMO orbital of SMX localizes around the N11, N17, N22 and O23 atoms with large electronegativity, which is easy to obtain electrons. Obviously, the negatively charged surface area is concentrated in the N22 and O23 atoms of the five-membered ring and the O15 and O16 regions where the π electron space extends. Therefore, the HOMO orbital region of SMX and the negatively charged region of ESP are easily attacked. According to EPR experiments and quenching experiments, HOCl, HOBr and $^1O_2$ are the main electrophilic reaction species, and free radicals (RO• and •OH) also play a certain role. The relatively large *f*-values follow the order of N11 (0.21943)>C3 (0.19242)>C1 (0.11613)>C5 (0.09078) (Table S4), and the f^0 values follow the order of C5 (0.158665)>N11 (0.12776)>C1 (0.11946)>C3 (0.095415), indicating that they are all susceptible to electrophilic and free radical attacks. Fig. S10 also proves that N11 and C5 are susceptible to electrophilic and free radical attacks, respectively. However, due to the saturated site and steric hindrance of C3, it is difficult to accept further

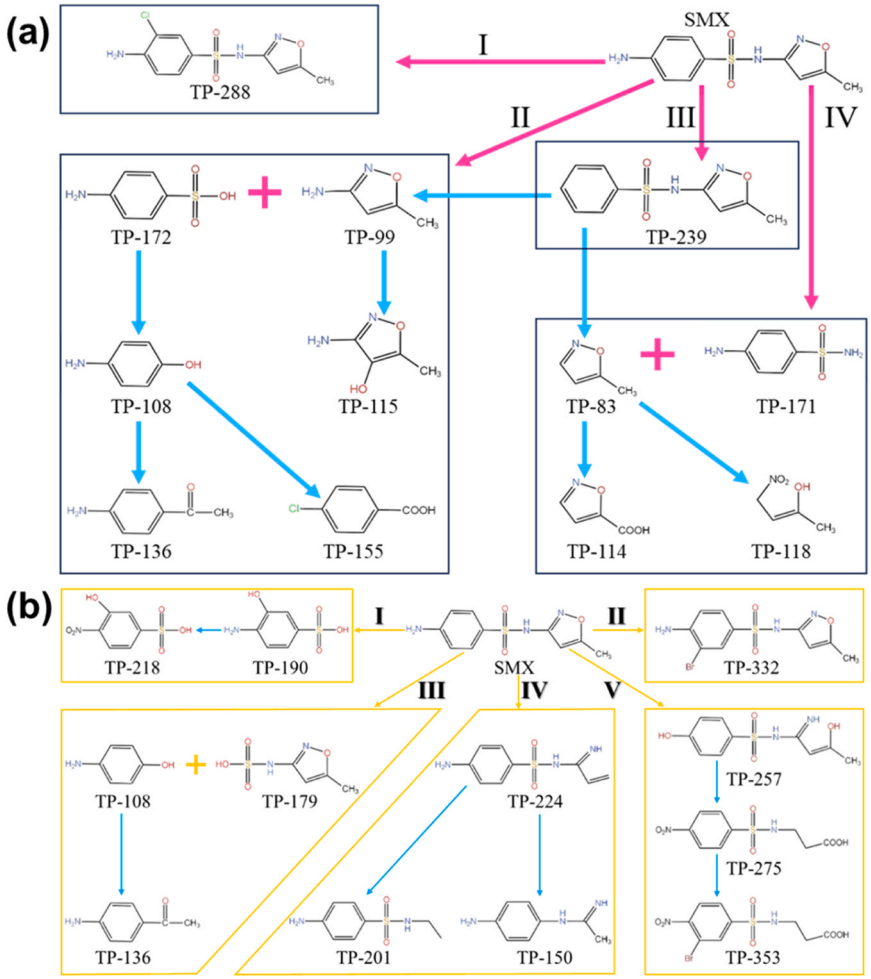

Fig. 9. (a) Mass spectra of SMX and its intermediates in Cl^--PAA system;(b) Mass spectra of SMX and its intermediates in Br^--PAA system.

[O] addition [57]. Therefore, this also proves that the Cl^-/Br^--PAA system degrades SMX mainly through electrophilic and free radical attacks.

Fig. S11 shows that TOC did not completely disappear, and the oxidation system had a low mineralization rate for SMX, indicating that there were still a large number of intermediates in the system. Based on the detection results of UPLC-TSQ-MS (Text S1,Tables S2 and S3) and frontier orbital theory calculations (Table S4 and S9), Fig. 9 proposed that the Cl^--PAA system had pathway I (chlorine substitution proved that free chlorine directly reacted with SMX, pathway II (S-N bond breaking, S-N bond has the lowest bond order and is easily attacked. It is worth noting that TP-108 undergoes chlorine substitution and carboxylation to form TP-155 in the presence of free chlorine and $^1O_2$), pathway III (deamination) and pathway IV (C-N bond breaking). Fig. 9 shows that the main reaction pathways of SMX in the Br-PAA system include pathway I (S-N bond breaking), pathway II (bromine substitution), pathway III (S-C bond breaking), pathway IV (isoxazole ring opening) and pathway V (hydroxylation).

3.6. Toxicity analysis

According to the Globally Harmonized System of Classification and Labeling of Chemicals (GHS), the ecotoxicity of SMX and its transformation products was systematically evaluated using the ECOSAR v2.2 program, with toxicity classifications categorized as: very toxic (LC50/EC50/ChV $\leq$1 mg·L^{-1}), toxic (1 −10 mg·L^{-1}), harmful (10 −100 mg·L^{-1}), and not harmful (> 100 mg·L^{-1}) [58]. The assessment predicted acute toxicity endpoints (96-h LC50 for fish and 48-h EC50 for daphnia) and chronic toxicity values (ChV for green algae), as summarized in Tables S5 and S6. The results demonstrated that SMX exhibited distinct toxicity profiles, showing toxic effects on Daphnia and harmful effects on green algae (Fig. 10), highlighting the need for careful consideration of its environmental impact and transformation products.

Some intermediates formed during the degradation process were predicted to have higher chronic toxicity than SMX, which may be due to the formation of more toxic pyrazole moieties. However, the toxicity of low molecular weight intermediates was significantly lower than that of their high molecular weight counterparts. This suggests that the toxicity of SMX can be effectively reduced by increasing the mineralization rate by extending the reaction time. Among the 12 SMX intermediates, TP-83, TP-108, TP-114, TP-155, TP-171, TP-172, and TP-239 had lower acute and chronic toxicity than SMX. In contrast, TP-99, TP-115, TP-118, TP-136, and TP-288 were predicted to have higher acute and chronic toxicity. Their high ecotoxicity was attributed to their presence of isoxazole or chlorine. In the Br^--PAA system, the acute toxicity was toxic and harmful to Daphnia and green algae, respectively, and the chronic toxicity was toxic and harmful to fish and green algae, respectively (Fig. S12). Most of the intermediates produced by SMX degradation showed higher acute/chronic toxicity than the parent compound, this indicates that the potential secondary pollution of sulfonamide antibiotics and their degradation intermediates deserves more attention.

4. Conclusion

This study provides the first systematic insight into the non-radical degradation mechanism of PAA activated via the synergistic action of Cl^- and Br^- in seawater systems, rather than within a single-halide system. The proposed technology enables efficient degradation of SMX without requiring external energy input, and exhibits strong tolerance across a wide pH range without the need for strict acidic conditions. The Br^--PAA system (0.5 mM Br^-) outperformed its Cl^--PAA counterpart (300 mM Cl^-), achieving complete SMX degradation within 12 min with a reaction rate constant 21-fold higher. Moreover, the degradation rate of sulfamethoxazole (SMX) in seawater with a salinity of 35 ‰ was significantly higher than that observed in systems containing only individual halides , while exhibiting robust resistance to common anion interference , thereby filling a critical knowledge gap in oxidation processes under high-salinity conditions that more closely mimic real aquatic environments. Mechanistic investigations through EPR and quenching experiments identified $^1O_2$ and free halogens as the dominant reactive species, generated directly via OAT, which demonstrated high selectivity for antibiotic degradation-albeit with the concurrent formation of more toxic transformation products. Furthermore, pH played a pivotal role in modulating oxidative pathways of the system: acidic to neutral conditions favored nonradical pathways (e.g., free halogens), whereas alkaline conditions shifted the balance toward OBr^-/OCl^-

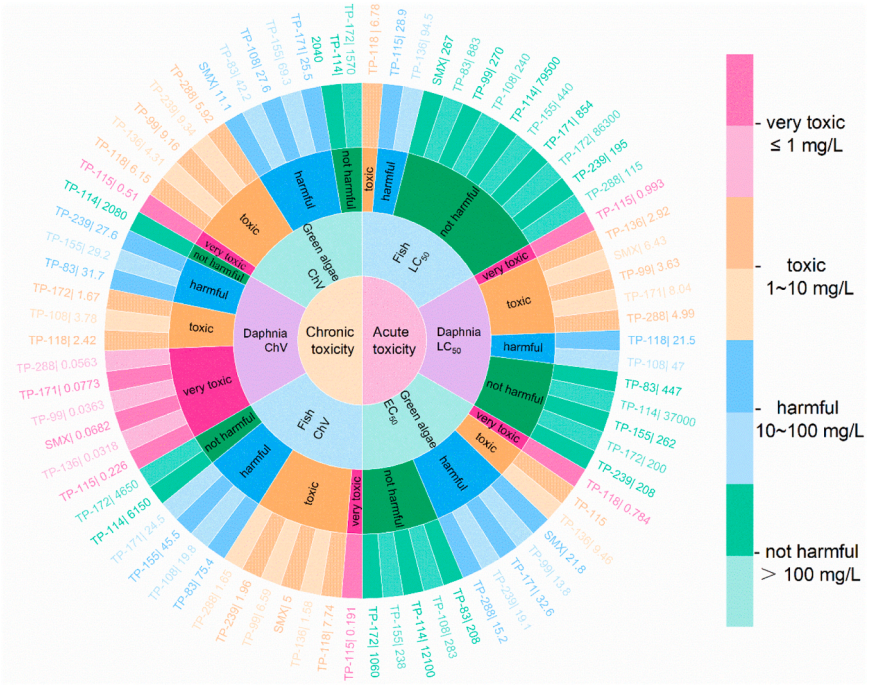

Fig. 10. Potential pathways of SMX's TPs generation in the Cl^--PAA system.

formation with partial radical involvement , These findings demonstrate the distinct roles of seawater-derived Cl^- and Br^- in PAA activation, with Br^- driving rapid oxidation while Cl^- contributes to secondary reaction pathways, highlighting their combined potential for saline wastewater treatment. These results provide valuable insights for the in situ remediation of antibiotic contamination in marine environments, facilitating the development of eco-friendly and low-cost marine pollution control technologies. In the future, this approach could be extended to the treatment of halogen-rich wastewater, such as effluents from mariculture and coastal industrial operations. As the present study was conducted under batch conditions, practical large-scale application would require further evaluation of equipment energy consumption and cost-effectiveness in continuous-flow reactors. Additionally, the potential formation of disinfection byproducts during long-term operation should be assessed.

CRediT authorship contribution statement

Jingzhen Su: Writing – original draft, Methodology, Data curation. **Yong Wang:** Data curation. **Cong Li:** Supervision, Funding acquisition, Conceptualization. **Zhengming He:** Software. **Kai Zhang:** Software. **Mingqiang Ren:** Investigation. **Qile Wang:** Investigation. **Tianxing Chen:** Investigation. **Jibran Ali Ghumro:** Investigation. **Virender K. Sharma:** Writing – review & editing. **Hyunook Kim:** Writing – review & editing, Funding acquisition. **Yunshu Zhang:** Writing – review & editing.

Declaration of Competing Interest

The authors declare that they have no known competing financial interests or personal relationships that could have appeared to influence the work reported in this paper.

Acknowledgments

This work was sponsored by the National Natural Science Foundation of China (Project No. 52442006) ,the Science and Technology Commission of Shanghai Municipality (Project No. 24DZ2306400 and the innovative drinking water and wastewater technologies project of Korea Environment Industry & Technology Institute (KEITI) (Project No. 2019002710006).

Appendix A. Supporting information

Supplementary data associated with this article can be found in the online version at doi:10.1016/j.jece.2025.119405.

Data availability

Data will be made available on request.

References

[1] L.L. Zhang, J.B. Chen, Y.L. Zhang, Y. Xu, T.L. Zheng, X.F. Zhou, Highly efficient activation of peracetic acid by nano-CuO for carbamazepine degradation in wastewater: the significant role of H_2O_2 and evidence of acetylperoxy radical contribution, Water Res. 216 (2022) 118322.
[2] X.W. Ao, J. Eloranta, C.H. Huang, D. Santoro, W.J. Sun, Z.D. Lu, C. Li, Peracetic acid-based advanced oxidation processes for decontamination and disinfection of water: a review, Water Res. 188 (2021) 116479.
[3] K.J. Zhang, X.Y. Zhou, P.H. Du, T.Q. Zhang, M.Q. Cai, P.Z. Sun, C.H. Huang, Oxidation of β-lactam antibiotics by peracetic acid: reaction kinetics, product and pathway evaluation, Water Res. 123 (2017) 153–161.
[4] S.K. Wu, R.C. Zhang, X.L. Fu, H. Zhang, P.Z. Sun, Reactivity of unactivated peroxymonosulfate and peroxyacetic acid with thioether micropollutants: mechanisms and rate prediction, Water Res. 256 (2024) 121601.
[5] B.Z. Liu, B.R. Huang, X.C. Ma, H.H. Huang, C. Zou, J.X. Liu, Q.Z. Luo, C. Wang, J. L. Liang, Recent advances in peracetic acid-based advanced oxidation processes for emerging pollutants elimination: a review, J. Environ. Chem. Eng. 12 (3) (2024) 112927.
[6] D. Kiejza, U. Kotowska, W. Polinska, J. Karpinska, Peracids-New oxidants in advanced oxidation processes: the use of peracetic acid, peroxymonosulfate, and persulfate salts in the removal of organic micropollutants of emerging concern-A review, Sci. Total Environ. 790 (2021) 148195.
[7] J.B. Chen, J. Xu, T.C. Liu, Q. Wang, N. Li, Y.L. Zhang, L.B. Yang, X.F. Zhou, Oxidation of tetracycline antibiotics by peracetic acid: reaction kinetics, mechanism, and antibacterial activity change, Chem. Eng. J. 431 (2022) 134190.
[8] S. Waclawek, H.V. Lutze, K. Grübel, V.V.T. Padil, M. Cerník, D.D. Dionysiou, Chemistry of persulfates in water and wastewater treatment: a review, Chem. Eng. J. 330 (2017) 44–62.
[9] J.W. Wang, Y. Wan, J.Q. Ding, Z.P. Wang, J. Ma, P.C. Xie, M.R. Wiesner, Thermal activation of peracetic acid in aquatic solution: the mechanism and application to degrade Sulfamethoxazole, Environ. Sci. Technol. 54 (22) (2020) 14635–14645.
[10] S.Q. Zhou, J.M. Huang, L.J. Bu, G.C. Li, S.M. Zhu, Degradation of β-N-methylamino-L-alanine (BMAA) by UV/peracetic acid system: influencing factors, degradation mechanism and DBP formation, Chemosphere 307 (2022) 136083–136091.
[11] Q. Zhang T, T. Wang, B. Mejia-Tickner, J. Kissel, X. Xie, C.H. Huang, Inactivation of bacteria by peracetic acid combined with ultraviolet irradiation: mechanism and optimization, Environ. Sci. Technol. 54 (15) (2020) 9652–9661.
[12] K.Y. Yao, L. Fang, P.B. Liao, H.S. Chen, Ultrasound-activated peracetic acid to degrade tetracycline hydrochloride: efficiency and mechanism, Sep. Purif. Technol. 306 (2023) 122635.
[13] T.D. Carlos, L.B. Bezerra, M.M. Vieira, R.A. Sarmento, D.H. Pereira, G.S. Cavallini, Fenton-type process using peracetic acid: efficiency, reaction elucidations and ecotoxicity, J. Hazard. Mater. 403 (2021) 123949.
[14] J.W. Wang, Z.P. Wang, Y.J. Cheng, L.S. Cao, F. Bai, S.Y. Yue, P.C. Xie, J. Ma, Molybdenum disulfide (MoS): a novel activator of peracetic acid for the degradation of sulfonamide antibiotics, Water Res. 201 (2021) 117291.
[15] J. Kim, P.H. Du, W. Liu, C. Luo, H. Zhao, C.H. Huang, Cobalt/peracetic acid: advanced oxidation of aromatic organic compounds by acetylperoxyl radicals, Environ. Sci. Technol. 54 (8) (2020) 5268–5278.
[16] B.H. Liu, W.Q. Guo, W.R. Jia, H.Z. Wang, Q.S. Si, Q. Zhao, H.C. Luo, J. Jiang, N. Q. Ren, Novel nonradical oxidation of sulfonamide antibiotics with Co(II)-doped g-CN-activated peracetic acid: role of high-valent cobalt-oxo species, Environ. Sci. Technol. 55 (18) (2021) 12640–12651.
[17] R.B. Li, K. Manoli, J. Kim, M.B. Feng, C.H. Huang, V.K. Sharma, Peracetic acid-ruthenium(III) oxidation process for the degradation of micropollutants in water, Environ. Sci. Technol. 55 (13) (2021) 9150–9160.
[18] Y. Huang, B. Sheng, Z.H. Wang, Q.Z. Liu, R.X. Yuan, D.X. Xiao, J.S. Liu, Deciphering the degradation/chlorination mechanisms of maleic acid in the Fe(II)/peroxymonosulfate process: an often overlooked effect of chloride, Water Res. 145 (2018) 453–463.
[19] L. Meng, J. Chen, D.Y. Kong, Y.F. Ji, J.H. Lu, X.M. Yin, Q.S. Zhou, Transformation of bromide and formation of brominated disinfection byproducts in peracetic acid oxidation of phenol, Chemosphere 291 (2022) 132698.
[20] Z. Wang, R. Yuan, Y. Guo, L. Xu, J. Liu, Effects of chloride ions on bleaching of azo dyes by Co^{2+}/oxone reagent: kinetic analysis, J. Hazard. Mater. 190 (1-3) (2011) 1083–1087.
[21] X.Y. Lou, Y.G. Guo, D.X. Xiao, Z.H. Wang, S.Y. Lu, J.S. Liu, Rapid dye degradation with reactive oxidants generated by chloride-induced peroxymonosulfate activation, Environ. Sci. Pollut. Res. 20 (9) (2013) 6317–6323.
[22] C.X. Li, C.B. Chen, Y.J. Wang, X.Z. Fu, S. Cui, J.Y. Lu, J. Li, H.Q. Liu, W.W. Li, T. C. Lau, Insights on the pH-dependent roles of peroxymonosulfate and chlorine ions in phenol oxidative transformation, Chem. Eng. J. 362 (2019) 570–575.
[23] Z.Z. Liu, Y. Fei, Z.C. Xia, R.J. Zhang, X. Chang, Y.F. Ji, D.Y. Kong, J.H. Lu, J. Chen, Insights into the oxidation of bisphenol a by peracetic acid enhanced with bromide: the role of free bromine, Sep. Purif. Technol. 302 (2022) 122159.
[24] Ministry of Ecology and Environment N D a R C, Ministry of Natural Resources, Ministry of Transport, Ministry of Agriculture and Rural Affairs, China Coast Guard. Notice on Issuing the 14th Five-Year Plan for Marine Ecological and Environmental Protection[EB/OL]. https://www.mee.gov.cn/xxgk2018/xxgk/xxgk03/202202/t20220222_969631.html, 2022, [25 August].
[25] Council T.S. Action Plan for Carbon Dioxide Peaking Before 2030[EB/OL]. https://www.gov.cn/gongbao/content/2021/content_5649731.htm, 2021, [25 August].
[26] B.L. Guo, J.Y. Wang, K. Sathiyan, X.M. Ma, E. Lichtfouse, C.H. Huang, V.K. Sharma, Enhanced oxidation of antibiotics by ferrate mediated with natural organic matter: role of phenolic moieties, Environ. Sci. Technol. 57 (47) (2023) 19033–19042.
[27] F.B. Dunn, A.I. Silverman, Sunlight photolysis of extracellular and intracellular antibiotic resistance genes and in photosensitizer-free water, Environ. Sci. Technol. 55 (16) (2021) 11019–11028.
[28] J.Y. Xiao, M.Y. Wang, Z.J. Pang, L. Dai, J.F. Lu, J. Zou, Simultaneous spectrophotometric determination of peracetic acid and the coexistent hydrogen peroxide using potassium iodide as the indicator, Anal. Methods 11 (14) (2019) 1930–1938.
[29] L.H. Qiu, C.X. Yan, Y. Zhang, Y.B. Chen, M.H. Nie, Hypochlorite-mediated degradation and detoxification of sulfathiazole in aqueous solution and soil slurry, Environ. Pollut. 350 (2024) 124039.
[30] L.L. Yang, L.F. Li, R.Y. Liu, C.G. Xie, J. Zhao, W.G. Chang, L.J. Chen, Y.H. Yan, N. N. Zhang, W. Zhang, B.H. Liu, L. Yang, Cationic fluorescent carbon dots with solution ultra-stability and its rapid/on-site sensing application for HClO, Talanta 267 (2024) 125137.
[31] M.B. Heeb, J. Criquet, S.G. Zimmermann-Steffens, U. von Gunten, Oxidative treatment of bromide-containing waters: formation of bromine and its reactions with inorganic and organic compounds-A critical review, Water Res. 48 (2014) 15–42.

[32] A.N. Wang, Z.C. Hua, Z.H. Wu, C.Y. Chen, S.D. Hou, B.J. Huang, Y.G. Wang, D. Wang, X.C. Li, C.A.H. Li, J.Y. Fang, Insights into the effects of bromide at fresh water levels on the radical chemistry in the UV/peroxydisulfate process, Water Res. 197 (2021) 117042.
[33] K. Kumar, D.W. Margerum, Kinetics and mechanism of General-Acid-Assisted oxidation of bromide by hypochlorite and hypochlorous Acid, Inorg. Chem. 26 (16) (1987) 2565–2736.
[34] A.D. Shah, Z.Q. Liu, E. Salhi, T. Höfer, U. von Gunten, Peracetic acid oxidation of saline waters in the absence and presence of H_2O_2: secondary oxidant and disinfection byproduct formation, Environ. Sci. Technol. 49 (3) (2015) 1698–1705.
[35] Z. Song, Y. Zhang, X. Zhang, X. Zhou, Y.D. Chen, X.G. Duan, N.Q. Ren, Kinetics study of chloride-activated peracetic acid for purifying bisphenol A: role of Cl/HClO and carbon-centered radicals, Water Res. 242 (2023) 120274.
[36] X. Yang, A.N. Wang, Z.C. Hua, W.R. Wei, Y.L. Cao, B.Y. Fu, S.P. Chen, Z.J. Dong, J. Y. Fang, Overlooked roles of Cl_2O and Cl_2 in micropollutant abatement and DBP formation by chlorination, Water Res. 229 (2023) 119449.
[37] S.Q. Zhou, J.M. Huang, L.J. Bu, G.C. Li, S.M. Zhu, Degradation of β-N-methylamino-L-alanine (BMAA) by UV/peracetic acid system: influencing factors, degradation mechanism and DBP formation, Chemosphere 307 (2022) 136083.
[38] Y.B. Li, J.Y. Qi, J.M. Shen, B.Y. Wang, J. Kang, P.W. Yan, Y.Z. Cheng, L. Li, L. L. Shen, Z.L. Chen, Non-radical dominated degradation of bisphenol s by peroxymonosulfate activation under high salinity condition: overlooked HOCl, formation of intermediates, and toxicity assessment, J. Hazard. Mater. 435 (2022) 128969.
[39] Y. Zhou, J. Jiang, Y. Gao, S.Y. Pang, J. Ma, J.B. Duan, Q. Guo, J. Li, Y. Yang, Oxidation of steroid estrogens by peroxymonosulfate (PMS) and effect of bromide and chloride ions: kinetics, products, and modeling, Water Res. 138 (2018) 56–66.
[40] L. Meng, J.Y. Dong, J. Chen, J.H. Lu, Y.F. Ji, Degradation of tetracyclines by peracetic acid and UV/peracetic acid: reactive species and theoretical computations, Chemosphere 320 (2023) 137969.
[41] H. Du P, W. Liu, M. Rao Z, J. Wang J, Accelerated oxidation of organic micropollutants during peracetic acid treatment in the presence of bromide ions, ACS EsT. Water 2 (2) (2022) 320–328.
[42] H. Tang, Q. Shang, Y. Tang, H. Liu, D. Zhang, Y. Du, C. Liu, Filter-membrane treatment of flowing antibiotic-containing wastewater through peroxydisulfate-coupled photocatalysis to reduce resistance gene and microbial inhibition during biological treatment, Water Res. 207 (2021) 117819.
[43] X. Tian, S. Liu, B. Zhang, S. Wang, S. Dong, Y. Liu, L. Feng, L. Zhang, Carbonized polyaniline-activated peracetic acid advanced oxidation process for organic removal: efficiency and mechanisms, Environ. Res. 219 (2023) 115035.
[44] Y.X. Huang, L.J. Bu, S.M. Zhu, S.Q. Zhou, Z. Shi, J.W. Wang, Dual role of bromide in the degradation of phenolic compounds in peracetic acid process: promotion of degradation and formation of disinfection byproducts, J. Environ. Chem. Eng. 10 (6) (2022) 108700.
[45] H.X. Zhao, L. Wang, D.Y. Kong, Y.F. Ji, J.H. Lu, X.M. Yin, Q.S. Zhou, Degradation of triclosan in a peroxymonosulfate/br system: identification of reactive species and formation of halogenated byproducts, Chem. Eng. J. 384 (2020) 123297.
[46] R.C. Troy, D.W. Margerum, Non-metal redox kinetics: hypobromite and hypobromous acid reactions with iodide and with sulfite and the hydrolysis of bromosulfate, Inorg. Chem. 30 (18) (1991) 3538–3543.
[47] L.S. Cao, J.W. Wang, Z.P. Wang, S.W. Yu, Y.J. Cheng, J. Ma, P.C. Xie, Inactivation of by peracetic acid combined with ultraviolet: performance and characteristics, Water Res. 208 (2022) 117847.
[48] Z.R. Wang, Y.S. Fu, Y.L. Peng, S.X. Wang, Y.Q. Liu, HCO_3^-/CO_3^{2-} enhanced degradation of diclofenac by Cu(II)-activated peracetic acid: efficiency and mechanism, Sep. Purif. Technol. 277 (2021) 119434.
[49] Z.P. Wang, Z.B. Chen, Q.B. Li, J.W. Wang, L.S. Cao, Y.J. Cheng, S.W. Yu, Z.Z. Liu, Y. Q. Chen, S.Y. Yue, J. Ma, P.C. Xie, Non-Radical activation of peracetic acid by powdered activated carbon for the degradation of sulfamethoxazole, Environ. Sci. Technol. 57 (28) (2023) 10478–10488.
[50] X.J. Lai, X.A. Ning, Y.P. Zhang, Y. Li, R.W. Li, J.Y. Chen, S.Y. Wu, Treatment of simulated textile sludge using the Fenton/Cl-system: the roles of chlorine radicals and superoxide anions on PAHs removal, Environ. Res. 197 (2021) 110997.
[51] P. Westerhoff, P. Chao, H. Mash, Reactivity of natural organic matter with aqueous chlorine and bromine, Water Res. 38 (6) (2004) 1502–1513.
[52] P.D. Hu, H.R. Su, Z.Y. Chen, C.Y. Yu, Q.L. Li, B.X. Zhou, P.J.J. Alvarez, M.C. Long, Selective degradation of organic pollutants using an efficient metal-free catalyst derived from carbonized polypyrrole via peroxymonosulfate activation, Environ. Sci. Technol. 51 (19) (2017) 11288–11296.
[53] R.D. Su, Y.X. Gao, L. Chen, Y. Chen, N. Li, W. Liu, B.Y. Gao, Q. Li, Utilizing the oxygen-atom trapping effect of Co_3O_4 with oxygen vacancies to promote chlorite activation for water decontamination, Proc. Natl. Acad. Sci. USA 121 (11) (2024) e2319427121.
[54] S.S. Zhu, X.J. Li, J. Kang, X.G. Duan, S.B. Wang, Persulfate activation on crystallographic manganese oxides: mechanism of singlet oxygen evolution for nonradical selective degradation of aqueous contaminants, Environ. Sci. Technol. 53 (1) (2019) 307–315.
[55] T.C. Liu, S.Z. Xiao, N. Li, J.B. Chen, Y. Xu, W.J. Yin, X.F. Zhou, C.H. Huang, Y. L. Zhang, Selective transformation of micropollutants in saline wastewater by peracetic acid: the overlooked brominating agents, Environ. Sci. Technol. 57 (47) (2023) 18940–18949.
[56] J.K. He, J.Y. Huang, Z.W. Wang, Z. Liu, Y. Chen, R.D. Su, X.Y. Ni, Y.W. Li, X. Xu, W. Z. Zhou, B.Y. Gao, Q. Li, The enhanced catalytic degradation of sulfamethoxazole over Fe@nitrogen-doped carbon-supported nanocomposite: insight into the mechanism, Chem. Eng. J. 439 (2022) 135784.
[57] P.P. Zamora, K. Bieger, A. Cuchillo, A. Tello, J.P. Muena, Theoretical determination of a reaction intermediate: fukui function analysis, dual reactivity descriptor and activation energy, J. Mol. Struct. 1227 (2021) 129369.
[58] Y.Y. Peng, W.H. Tong, Y. Xie, W.R. Hu, Y.H. Li, Y.K. Zhang, Y.B. Wang, Yeast biomass-induced Co_2P/biochar composite for sulfonamide antibiotics degradation through peroxymonosulfate activation, Environ. Pollut. 268 (2021) 115930, 115938.